Rheological Characterization of Carbon Black/Polystyrene Solution Systems

Yuji Aoki

Department of Polymer Science and Engineering, Yamagata University, Yonezawa, Yamagata 992-8510, Japan

Received 4 September 2006; accepted 3 October 2007
DOI 10.1002/app.27650
Published online 21 February 2008 in Wiley InterScience (www.interscience.wiley.com).

ABSTRACT: Steady-shear measurements of suspensions of carbon blacks (CB) in polystyrene (PS)/di-(butyl phthalate) (DBP) solution were investigated as a function of volume fraction (ϕ) of CB to clarify the effect of the primary particle size and the structure of CB aggregates on the rheological properties. The suspensions show a typical shear-thinning behavior in the range of a shear rate studied. The Casson model was applied to evaluate the viscosity at infinite of shear rate η_∞ and the yield stress σ_y for the suspensions. Relative viscosity η_∞/η_m, (η_m: medium viscosity) thus obtained was compared to the high-frequency viscosity for the ideal hard-sphere silica suspensions to evaluate the effective volume fraction ϕ_{eff} of CB aggregates. The ϕ_{eff} value was larger for the higher-structure CB with higher DBP absorption value, irrespective of the primary particle size. The yield stress σ_y had almost the same ϕ_{eff} dependence for neutral furnace CB/(PS/DBP) suspensions, although it was larger for acetylene black (AcB)/(PS/DBP) suspensions. These results demonstrated that the effective volume fraction is the most important quantity to characterize the CB aggregates on the rheological properties. It was also found that the correction of the medium viscosity changes due to polymer adsorption on the CB surface is important since neutral furnace CB adsorbs PS polymers but AcB hardly adsorbs PS polymers in the solution. © 2008 Wiley Periodicals, Inc. J Appl Polym Sci 108: 2660–2666, 2008

Key words: carbon black; polystyrene solution; rheology; steady shear; network structure

INTRODUCTION

Carbon black (CB) is widely used as a reinforcing agent in rubber products and as an additive for pigmentation, UV protection, electrical conductivity, and rheology control in plastics, ink, and coating. Rheological properties of CB/polymer compounds and CB suspensions are very important from both academic and industrial points of view. In attempting to elucidate these rheological responses, extensive studies have been carried out for the CB/polymer compounds[1–11] and CB suspensions.[12–30] The occurrence of both yield stress and thixotropy for these systems has been found. In general, an increase in the CB concentration and a decrease in the particle size enhance the agglomerate formation thereby increase the viscosity.

CB is constituted of carbon primary particles fused by covalent bonds into aggregates that generally are considered unbreakable during the normal processing of the materials.[31] The CB aggregates exist in a variety of shape types from the higher-structure CB grades consisting of more branched structures to the lower structure grades containing more compact structures. The aggregates have a strong tendency to agglomerate because of the electronic structure of the CB surface. In contrast to the aggregates, these agglomerates are characterized by weak bonding between the aggregates and therefore do not retain their integrity during processing. Therefore, the rheological properties might change with not only the CB agglomerate structure, but also the aggregate structure. However, there were few studies concerning the relationship between the rheological properties and the CB aggregate structure, although it was reported that the type of CB has a significant influence on the rheological behavior[7] and the electrical conductivity of CB/rubber systems.[32]

Recently, we studied the dynamic viscoelastic properties of the CB suspensions and found that the rheological behavior of the CB suspensions changes with the affinity of suspending medium toward the CB particles and is classified into three different types of the behavior as summarized below.[27] In the medium having a poor affinity for the CB particles, the CB particles form well-developed network-like agglomerates. This strongly flocculated network structure exhibits highly nonlinear, elasto-plastic features. These CB agglomerates are unable to rearrange within laboratory time scales; hence the structures cannot relax to achieve thermodynamic equilibrium. This nonequilibrium structure of strongly flocculated gels would affect suspension property by increasing elasticity and viscosity. As we reported

Correspondence to: Y. Aoki (y.aoki@yz.yamagata-u.ac.jp).

Journal of Applied Polymer Science, Vol. 108, 2660–2666 (2008)

previously,[27] for the well-developed network-like CB aggregates, the apparent storage and loss moduli G'_{app} and G''_{app} for very small strain amplitude γ_0 (<0.3%) are independent of γ_0 and the linear viscoelastic behavior prevails. However, for larger γ_0 (>0.3%), the apparent moduli (in particular G'_{app}) continuously decrease with increasing γ_0. When a suspension exhibits such a strong nonlinearity due to the elasto-plastic deformation/flow of the network-type agglomerate, dynamic oscillation methods are not suitable. To characterize these strongly flocculated CB aggregates, steady shear measurements are suitable and can provide interesting rheological quantities, such as a flow curve and a yield stress. Accordingly, many studies have been made for these systems by the steady-state shear measurements, as shown before. However, most of the literatures on the topic of rheological properties of CB compounds and suspensions have focused on the concentration dependence of CB particles. The effects of CB aggregates on the rheological properties for these CB systems have not been fully elucidated, although such studies are very important and useful not only for the design of CB suspensions, but also for that of polymer/CB compounds.

Considering this program, we prepared the CB suspensions in polystyrene (PS)/di-(butyl phthlate) (DBP) solution using CB samples having different kinds of ''aggregate'' structure with various CB contents, and conducted steady-shear measurements of the suspensions. The yield stress σ_y and the viscosity at infinite of shear rate η_∞ were evaluated using the Casson model.[33] The relationship between these rheological quantities and the structure of CB aggregates is discussed in terms of an effective volume fraction ϕ_{eff} of CB aggregates. This is the first report to clarify the importance of the CB aggregate structure on the rheological properties. Effects of polymer adsorption on the rheological properties are also discussed.

EXPERIMENTAL

Four series of carbon black (CB-76, CB-24-1, CB-15-2, and AcB) suspensions with various CB concentrations c_{CB} in PS/DBP solution were used in this study. CB-76, CB-24-1, and CB-15-2, supplied from Mitsubishi Chemical Corp. (Japan), were formed by oil furnace process. AcB was an acetylene black type CB supplied from Denki Kagaku Kogyou Co. (Japan). Characteristics of these CB samples are shown in Table I. Surface area is a measure of particle size, and was measured by absorption of nitrogen gas onto the carbon black. DBP absorption is a measure of aggregate size and was measured as following; a quality of CB is placed in the mixing chamber of torque-measuring electric kneader-mixer. The kneader action is started and DBP is added drop-wise from an automatic burette. The transition from a free-flowing powder to a semiplastic material at the point of maximum absorption (the filling of voids) results in a rapid rise in torque, which activates an automatic cutoff in burette and kneader. The volume of DBP added is registered automatically. Its value per 100 g of CB, the DBP number, is a reproducible quantity recognized as a structural index in ASTM method D2415-65T. Aggregates with a greater number of particles and more complex aggregates (higher structure CB) have more voids and thus have a higher oil demand. Accordingly, CB-76 and CB-24-1 have almost the same DBP absorption value and are lower structure grades consisting of more compact aggregates. CB-15-2 is higher structure grades containing more branched aggregates. AcB has the highest DBP absorption value among CB samples studied here, although the primary particle size is not the smallest.

TABLE I
Characteristics of CB Samples

Carbon black	CB-76	CB-24-1	CB-15-2	AcB
Mean particle size (nm)	76	24	15	40
Surrface area (m^2/g)	29	130	294	61
Average aggregate size (nm)	230	180	210	350
DBP absorption value (mL/100 g)	71	69	147	190
ϕ_{eff}/ϕ	2.6	2.6	5.5	16

The suspensions were prepared by mixing known amounts of dry CB with 5 wt % PS/DBP solution (disperse medium). CB concentration c_{CB} measured depended on CB species because of different aggregate structure, and was ranged from 0 to 20 wt % for CB-76 suspension, to 22.5 wt % for CB-24-1, to 10 wt % for CB-15-2 suspension, and to 3 wt % for AcB suspension. For these suspensions, steady-shear measurements were carried out with a rheometer (ARES, Rheometrics) at 25°C. Cone-plate fixtures with a gap angle of 0.0845 rad and a plate diameter of 25 and/or 50 mm were used.

RESULTS AND DISCUSSION

Flow curves and Casson plots

Figure 1(a–d) shows the shear rate $\dot{\gamma}$ dependence of the steady shear viscosity η of the CB-76 (a), CB-24-1 (b), CB-15-2 (c), and AcB (d) suspensions having various CB concentrations c_{CB}. The suspending medium (PS/DBP solution) shows a constant viscosity independent of $\dot{\gamma}$ and exhibits a Newtonian flow. On the other hand, all the CB/(PS/DBP) suspensions are characterized by a typical shear thinning behavior.

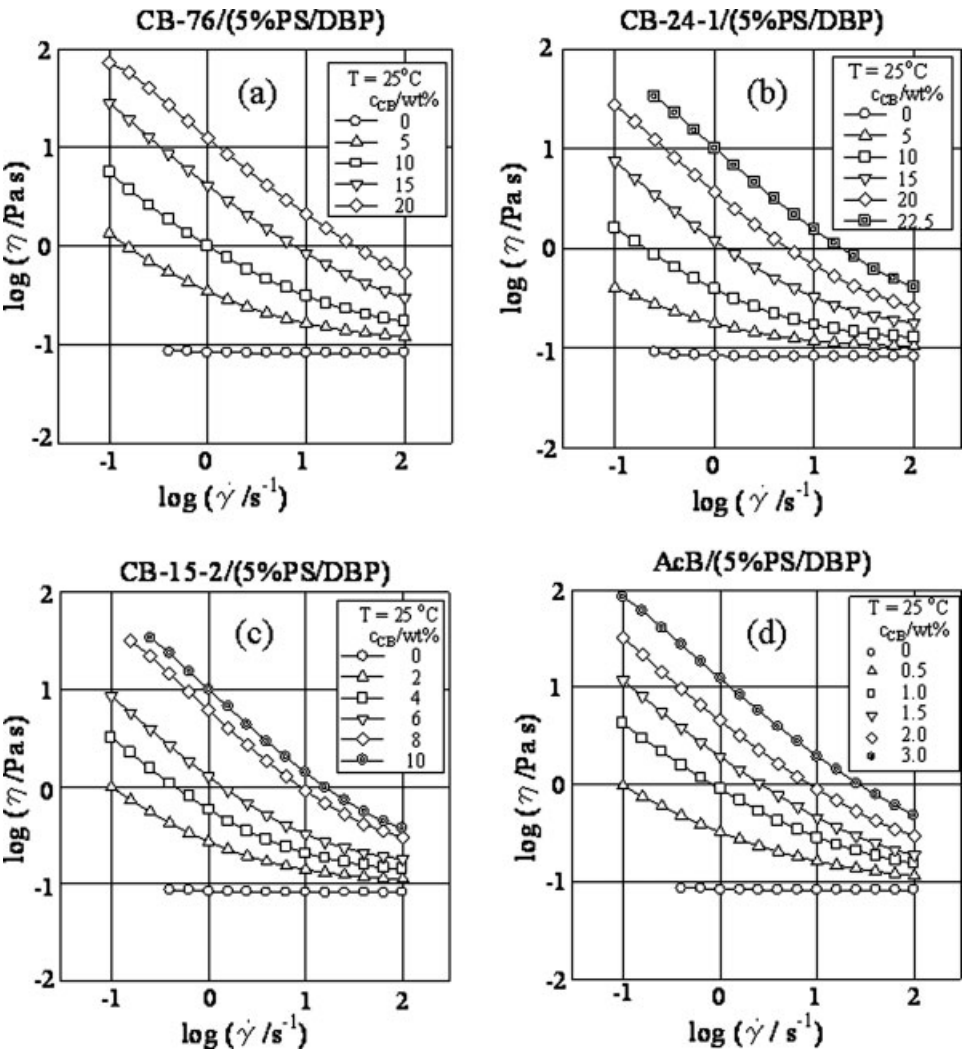

Figure 1 Flow curves of the CB-76/(5%PS/DBP) (a), CB-24-1(5%PS/DBP) (b), CB-15-2/(5%PS/DBP) (c), and AcB/(5%PS/DBP) (d) suspensions at 25°C.

The viscosities seem to approach to a constant viscosity at high shear rate. Both the degree of shear thinning and the viscosity at high shear rate increased with increasing c_{CB}. The shapes of the flow curve were very similar, although the correspondence c_{CB} was different for each suspension.

Casson[33] presented the following equation, which is now called the Casson equation. This equation has been applied to many kinds of suspensions and found to be useful.

$$\sigma^{1/2} = k_0 + k_1\dot{\gamma}^{1/2} \quad (1)$$

The Casson equation was derived under an assumption that the dispersed particles are agglomerated in the rod shape and the rods are destroyed in a small size under external shear field. This assumption can be applied to the CB suspensions because the agglomerate structure consisting of CB aggregates corresponds to the rods and the rod structure should be destroyed in smaller agglomerates under high shear. At very high shear, the rods must be divided to CB aggregates, as Onogi et al. reported that the Casson equation can be applied to the CB suspensions.[13–15,17] Using the Casson equation, we evaluated the yield stress σ_y and the viscosity at infinite of shear rate η_∞ of the suspensions. Here, the yield stress σ_y $(=k_0^2)$ was obtained by extrapolation at the shear rate $\dot{\gamma} = 0$. The viscosity at infinite of shear rate η_∞ was obtained from the slope of Casson plot. As a representative example, the Casson plots for the CB-24-1/(PS/DBP) are shown in Figure 2. Linearity in all the $\sigma^{1/2} - \dot{\gamma}^{1/2}$ relationships is evident at higher shear rate, although the stress decreased at low shear rates for higher c_{CB} samples, as already pointed out by Onogi and Matsumoto.[17] These results indicate that the yield values estimated from Casson plot may lead to an overestimation. However, the values thus evaluated would be a meaningful parameter to characterize CB

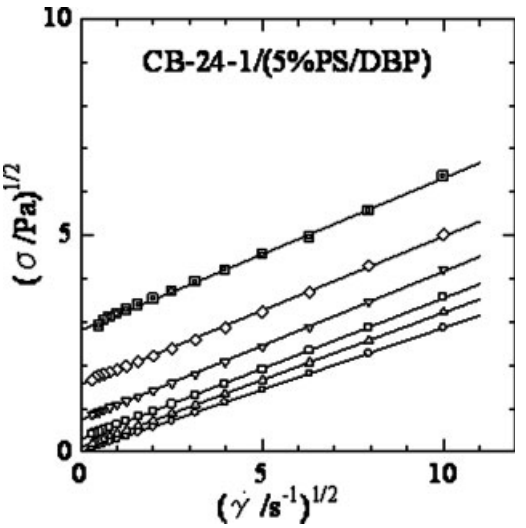

Figure 2 Casson plots of the CB-24-1/(5%PS/DBP) suspensions at 25°C. The symbols are the same as in Figure 1.

aggregates. Similar Casson plots could be obtained for the other three suspensions. From the basic concept of the Casson model, such linearity provides a strong evidence of the presence of connected CB aggregate networks in the CB suspensions.

Medium viscosity change due to CB aggregates

It has been reported that, for some suspensions in polymeric solutions, polymer chains are adsorbed on the particles to enhance the network-like agglomeration of the particles.[34–36] If the CB aggregates also adsorb PS in the PS/DBP solution, the medium viscosity η_m must change. To analyze relative viscosity η_r ($=\eta_\infty/\eta_m$) versus volume fraction ϕ relationship, the medium viscosity η_m for the suspensions was measured. The CB suspensions were centrifuged at 18,000 rpm for 2 h. The supernatant solution after centrifugation was transparent for all the suspensions and was considered not to contain any CB particles, accordingly. Table II shows the viscosity of the three series of supernatant solutions after centrifugation. The viscosity of the supernatant solutions decreased with c_{CB} for the CB-76/(PS/DBP), CB-24-1/(PS/DBP), and CB-15-2/(PS/DBP) suspensions, whereas the viscosity of the AcB/(PS/DBP) suspension was almost constant irrespective of c_{CB}, although the data were not tabulated here. These results indicate that PS molecules were adsorbed on the surface of the neutral furnace blacks (CB-76, CB-24-1, and CB-15-2). The amount of adsorbed PS could be estimated, as it was found that the log viscosity of the PS/DBP solution increases with weight fraction of PS. The amount of adsorbed PS thus estimated was 24 mg/(g of CB) for the CB-76 suspensions, 77 mg/(g of CB) for the CB-24-1 suspensions, and 124 mg/(g of CB) for the CB-15-2 suspensions, but almost 0 mg/(g of CB) for the AcB suspensions.

The PS concentration in the supernatant solutions was found to be lower than the original concentration (5 wt %). Thus, it is clear that the PS chains are adsorbed on the CB aggregates. Furnace CB aggregates typically contain about 90–99% elemental carbon, with oxygen and hydrogen as the other major constituents.[26] The oxygen and hydrogen of the furnace CB surface may prove the adsorption of the PS onto the CB aggregates. On the other hand, AcB contains almost 100% elemental carbon and is constructed of a graphite structure. Our experimental data indicate that the graphite structure never adsorbs the PS chains. However, the flow curves of the AcB suspensions are very similar to those of the furnace black suspensions.

High-shear relative viscosity

Figure 3(a,b) shows the bare volume fraction ϕ dependence of the high-shear relative viscosity $\eta_r = \eta_\infty/\eta_m$ for the CB-76 (a) and CB-15-2 (b) suspensions. Here, the bare volume fraction ϕ of the CB was calculated using the densities of CB ($\rho = 1.9$) and PS/DBP solution ($\rho = 1.05$). In these figures, filled circles denote the uncorrected data using the viscosity of 5% PS/DBP and open circles the corrected data using the viscosity of the supernatant solutions as η_m. As shown in the previous section, the medium viscosity η_m decreased with increasing CB concentration. Accordingly, the corrected values had higher ϕ dependence, because of low η_m. It is clear that the correction gives a significant difference for the ϕ dependence of the relative viscosity η_r. Therefore, we would like to emphasize that the adsorbed PS molecules strongly affect the suspension viscosity by changing the polymer concentration.

Figure 4 shows the ϕ dependence of the relative viscosity η_r for the CB-76, CB-24-1, CB-15-2, and AcB suspensions. It is clear that the CB suspensions with larger DBP absorption value have larger ϕ dependence. Why do these suspensions have different ϕ dependence? To explain the reason, we utilized effective volume fraction ϕ_{eff} instead of bare volume

TABLE II
The Viscosity of Supernatant Solutions for the CB-76/(PS/DBP), CB-24-1/(PS/DBP), and CB-15-2/(PS/DBP) Suspensions

CB-76 wt %	η (Pa s)	CB-24-1 wt %	η (Pa s)	CB-15-2 wt %	η (Pa s)
0	0.0787	0	0.0787	0	0.0787
5	0.0761	5	–	4	0.0716
10	0.0736	10	0.0630	8	0.0589
15	0.0714	15	0.0533	12	0.0481

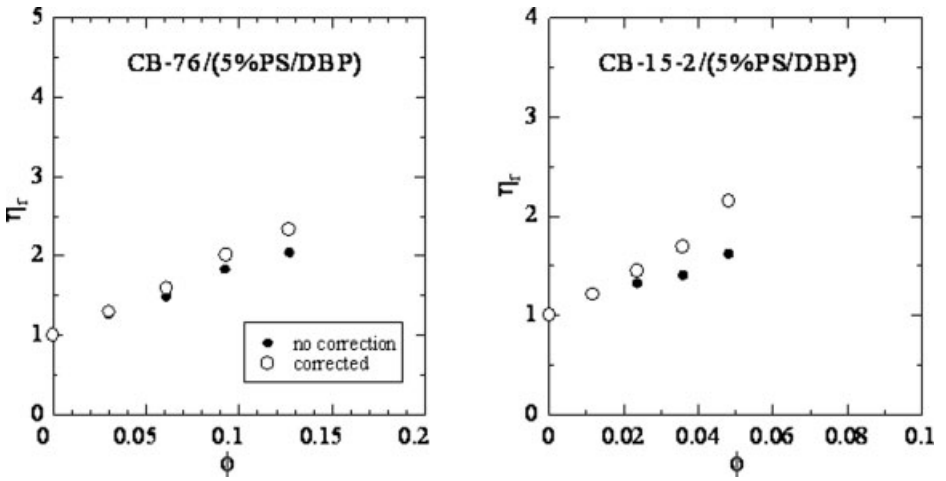

Figure 3 Relative viscosity η_r versus volume fraction ϕ plots of the CB-76/(5%PS/DBP) (a) and CB-15-2/(5%PS/DBP) (b) suspensions. Filled small circles denote the uncorrected values and open circles the corrected values by polymer adsorption.

fraction ϕ of the CB aggregates, as reported in our previous papers.[27,28] CB aggregates have nonspherical and nonuniform shape. Therefore, the effective volume fraction ϕ_{eff} would be larger than the bare volume fraction ϕ. Moreover, the CB aggregates must trap and/or adsorb the PS solution. This ''dead'' PS solution looses its identity as a solution and behaves as a part of filler in terms of the rheological behavior. These are the reason why the bare volume fraction ϕ is converted to the effective volume fraction ϕ_{eff}. The ϕ_{eff} must include both effects due to the shape of CB aggregates and immobilized PS solutions on the CB surface.

The effective volume corresponds to a volume occupied by sphere having the aggregate radius *a*. The ϕ_{eff} value was estimated as follows; for monodisperse hard-core silica suspensions, the high frequency viscosity η'_∞ normalized by the medium viscosity η_m is universally dependent on ϕ irrespective of the particle radius.[37,38] We evaluated the ϕ_{eff} of our CB aggregates ($\phi_{eff} = \alpha\phi$) by comparing the η_∞/η_m ratios of the CB aggregates and the universal η'_∞/η_m versus ϕ curve for the hard-core silica particles. The result is shown in Figure 5. From the abscissa coordinates of the plot for the CB aggregates (open symbols), the α value was estimated to be 2.6, 2.6, 5.5, and 16 for the CB-76, CB-24-1, CB-15-2, and AcB suspensions, respectively. This result indicates that the α value or the effective volume is an important parameter to characterize CB aggregates.

With increasing shear rate, the density of the three-dimensional network of the CB aggregates is decreased. Under sufficient high shear, the size of flow unit becomes the CB aggregate size. In this shear region, the second Newtonian flow appears. Therefore, the CB aggregates are considered to be a flow unit corresponding to ''effective volume''. The α value increases with increasing the DBP absorption value, suggesting that ϕ_{eff} depends mainly on aggregate structure morphology irrespective of particle size. This result indicates that the CB aggregates behave as a flow unit at high shear rates and the difference between ϕ_{eff} and ϕ reflects mainly the nonspherical shapes of the aggregates.

Yield stress

Figure 6 shows the yield stress σ_y of the CB-76, CB-24-1, CB-15-2, and AcB suspensions as a function of bare volume fraction ϕ. The σ_y of these suspensions changed drastically at a certain critical concentration,

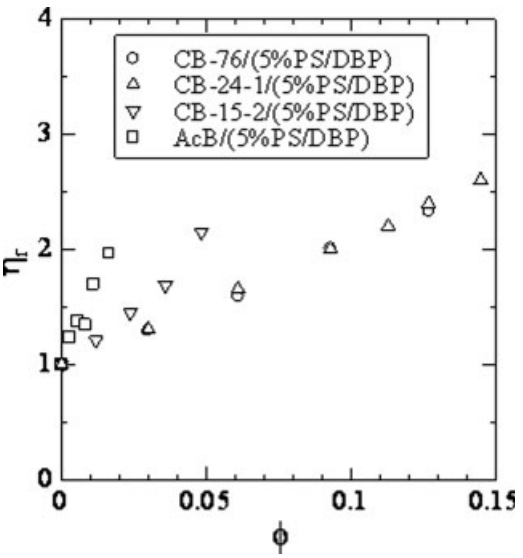

Figure 4 Relative viscosity η_r versus volume fraction ϕ plots of the CB-76/(5%PS/DBP), CB-24-1/(5%PS/DBP), CB-15-2/(5%PS/DBP), and AcB/(5%PS/DBP) suspensions.

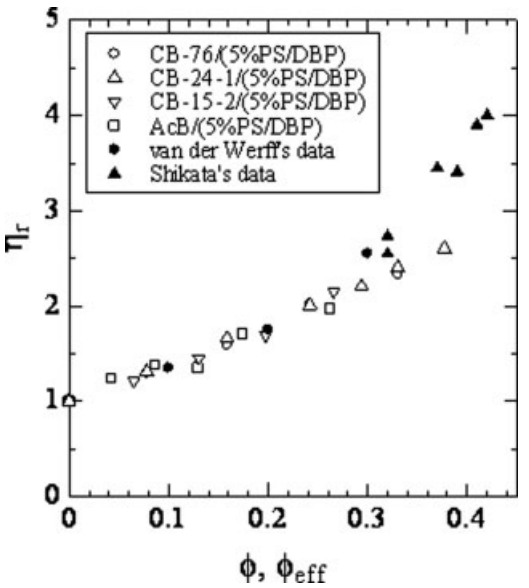

Figure 5 Relative viscosity η_r versus effective volume fraction ϕ_{eff} plots of the CB-76/(5%PS/DBP), CB-24-1/(5%PS/DBP), CB-15-2/(5%PS/DBP), and AcB/(5%PS/DBP) suspensions. The ϕ_{eff} values were determined in a way that the η_∞/η_m versus ϕ_{eff} for four suspensions were superposed on the universal η'_∞/η_m versus ϕ plots obtained for unimodal hard-core particles.[37,38]

ϕ_g, which corresponds to the formation of a space-filling network. At $\phi < \phi_g$, dilute suspensions have no yield stress and the discrete clusters settle in the dilute suspensions rather independently. Whereas above ϕ_g, the suspensions develop a three-dimensional network structure of the CB aggregates therein.

The yield stress σ_y is a force produced by the separation between the particles times the number of interparticle bonds that cross a unit area of the sample[39]: The latter factor is scaled as ϕ^2/a^2, where ϕ is particle volume fraction and a particle radius.[40] For our CB suspension systems, we used the average aggregate radius as a, and used the effective volume fraction ϕ_{eff} instead of ϕ, as same as we analyzed the high-shear relative viscosity in the previous section. In Figure 7, the σ_y data of the CB suspensions were normalized by $(a/a_0)^2$ and plotted against ϕ_{eff}, where a_0 = 100 nm. It was found that these plots also agreed with each other for the three furnace black (CB-76, CB-24-1, and CB-15-2) suspensions. We can conclude that the σ_y is attributed to some internal structures formed by CB aggregates and the stress to break up into CB aggregates must be almost the same for the furnace black samples.

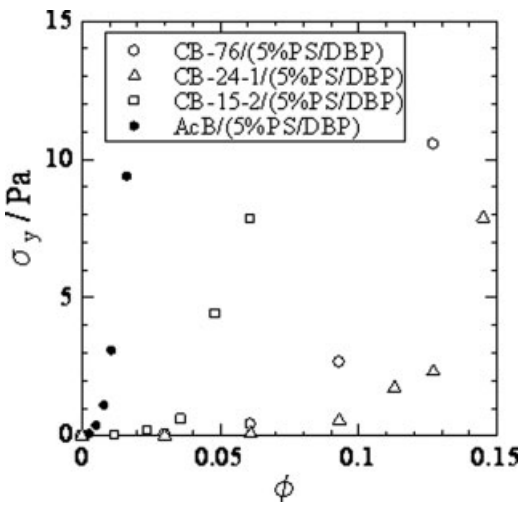

Figure 6 Yield stress σ_y versus volume fraction ϕ plots of the CB-76/(5%PS/DBP), CB-24-1/(5%PS/DBP), CB-15-2/(5%PS/DBP), and AcB/(5%PS/DBP) suspensions.

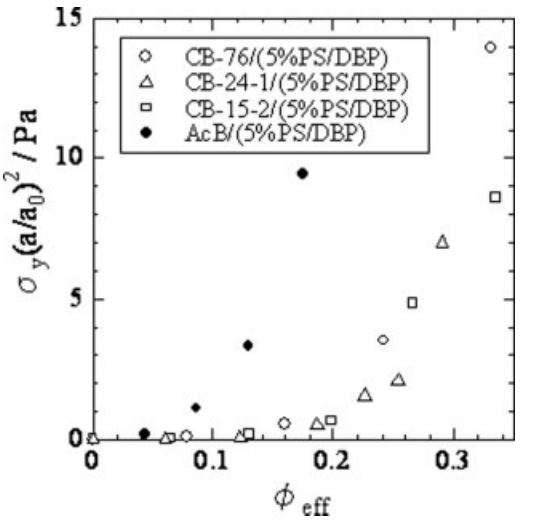

Figure 7 Yield stress σ_y versus effective volume fraction ϕ_{eff} for the CB-76/(5%PS/DBP), CB-24-1/(5%PS/DBP), CB-15-2/(5%PS/DBP), and AcB/(5%PS/DBP) suspensions. a_0 = 100 nm.

Finally, we mention briefly the reasons why the σ_y values of the AcB suspensions were larger than those of CB-76, CB-24-1, and CB-15-2 suspensions. The surface of AcB develops a graphite structure, although that of the furnace black does not. The surface structure difference may be attributed to different PS adsorption behavior and the ϕ_{eff} dependence of the σ_y values, although we cannot explain the mechanism yet.

CONCLUSIONS

We studied details of the steady-shear behavior of the CB/(PS/DBP) suspensions forming well-developed network-like CB agglomerates. The Casson model was applied to evaluate the yield stress σ_y and the viscosity at infinite of shear rate η_∞ for the suspensions. The effective volume fraction ϕ_{eff} was evaluated from the comparison with the universal η'_∞/η_m versus ϕ curve for the hard-core silica

particles, and found to depend strongly on the CB aggregate structure (DBP absorption value). It was found that the ϕ_{eff} is an important parameter to characterize the CB aggregates. The σ_y was found to be only a function of ϕ_{eff} irrespective of CB aggregate structure for the furnace black, but to be larger for the acetylene black sample. This may be due to the difference in the surface structure of CB and accordingly polymer adsorption behavior.

The author would like to express his thanks to Ms. Ayumi Aoki for improvement of the manuscript.

REFERENCES

1. Mullins, L. J Phys Colloid Chem 1950, 54, 539.
2. Mullins, L.; Whorlow, R. W. Trans Inst Rubber Ind 1951, 27, 55.
3. Vinogradov, G. V.; Malkin, A. Y.; Plotnikova, E.; Sabsai, O. Y.; Nikolayeva, N. E. Int J Polym Mater 1972, 2, 1217.
4. Lobe, V. M.; White, J. L. Polym Eng Sci 1979, 19, 617.
5. Montes, S.; White, J. L. Polym Eng Sci 1982, 55, 1359.
6. Song, H. J.; White, J. L.; Min, K.; Nakajima, N.; Weissert, F. C. Adv Polym Technol 1988, 8, 431.
7. Montes, S.; White, J. L.; Nakajima, N. J Non-Newtonian Fluid Mech 1988, 28, 183.
8. Gandhi, K.; Salovey, R. Polym Eng Sci 1988, 28, 877.
9. Shin, K. C.; White, J. L.; Brzoskowski, R.; Nakajima, N. Kautsch Gummi Kunstst 1990, 43, 181.
10. Montes, S.; White, J. L. J Non-Newtonian Fluid Mech 1993, 49, 277.
11. Osanaiye, G. J.; Leonov, A. I.; White, J. L. J Non-Newtonian Fluid Mech 1993, 49, 87.
12. Seno, M. Nippon Kagaku Zasshi 1957, 78, 66.
13. Onogi, S.; Masuda, T.; Matsumoto, T. Nippon Kagaku Zasshi 1967, 88, 854.
14. Onogi, S.; Masuda, T.; Matsumoto, T. Nippon Kagaku Zasshi 1968, 89, 464.
15. Matsumoto, T.; Masuda, T.; Tsutsui, K.; Onogi, S. Nippon Kagaku Zasshi 1969, 90, 360.
16. Schoukens, G.; Mewis, J. J Rheol 1978, 22, 381.
17. Onogi, S.; Matsumoto, T. Polym Eng Rev 1981, 1, 45.
18. Amari, T.; Watanabe, K. Polym Eng Rev 1983, 3, 277.
19. Amari, T.; Watanabe, K. Nihon Reoroji Gakkaishi 1986, 14, 37.
20. Amari, T.; Watanabe, K. J Rheol 1990, 34, 207.
21. Hayashi, T.; Morita, K.; Tateiri, M.; Amari, T. J Jpn Soc Colour Mater 1994, 67, 80.
22. Ishii, C.; Akao, K.; Koseki, K.; Amari, T. J Jpn Soc Color Mater 1997, 70, 584.
23. Amari, T.; Uesugi, K.; Suzuki, H. Prog Org Coat 1997, 31, 171.
24. Trappe, V.; Weitz, D. A. Phys Rev Lett 2000, 85, 449.
25. Kawaguchi, M.; Okuno, M.; Kato, T. Langmuir 2001, 17, 6041.
26. Lin, Y.; Smith, T. W.; Alexandridis, P. Langmuir 2002, 18, 6147.
27. Aoki, Y.; Hatano, A.; Watanabe, H. Rheol Acta 2003, 42, 209.
28. Aoki, Y.; Hatano, A.; Watanabe, H. Rheol Acta 2003, 42, 321.
29. Aoki, Y.; Watanabe, H. Rheol Acta 2004, 43, 390.
30. Won, Y.-Y.; Meeker, S. P. Trappe, V.; Weitz, D. A.; Diggs, N. Z.; Emert, J. I. Langmuir 2005, 21, 924.
31. Hagerstrom, J. In Polymers, Laminations and Coatings Conference; 1998; p 553.
32. Donnelly, P. J. Pap Meet Rubber Div Am Chem Soc 2000, 158, 1.
33. Casson, N. Rheology of Disperse Systems; Pergamon Press: New York, 1959; p 84.
34. Iler, K. R. J Colloid Interface Sci 1971, 37, 364.
35. Otsubo, Y. J Colloid Interface Sci 1992, 153, 584.
36. Otsubo, Y. J Rheol 1993, 37, 799.
37. Shikata, T.; Pearson, D. S. J Rheol, 1994, 38, 601.
38. van der Werff, J.C.; de Kruif, C. G.; Blom, C.; Mellema, J. Phys Rev A 1989, 39, 795.
39. Larson, R. G. The Structure and Rheology of Complex Fluids; Oxford University Press: New York, 1999.
40. Russel, W. B.; Saville, D. A.; Schowalter, W. R. Colloidal Dispersions; Cambridge University Press: Cambridge, 1989.